REPORT DOCUMENTATION PAGE

Form Approved
OMB No. 0704-0188

1. REPORT DATE *(DD-MM-YYYY)* 01 July 2016	**2. REPORT TYPE** Briefing Charts	**3. DATES COVERED** *(From - To)* 07 June 2016 - 01 July 2016

4. TITLE AND SUBTITLE The Blended Finite Element Method for Multi-fluid Plasma Modeling	**5a. CONTRACT NUMBER**
	5b. GRANT NUMBER
	5c. PROGRAM ELEMENT NUMBER
6. AUTHOR(S) Eder M. Sousa and Uri Shumlak	**5d. PROJECT NUMBER**
	5e. TASK NUMBER
	5f. WORK UNIT NUMBER Q1AM
7. PERFORMING ORGANIZATION NAME(S) AND ADDRESS(ES) Air Force Research Laboratory (AFMC) AFRL/RQRS 1 Ara Drive Edwards AFB, CA 93524-7013	**8. PERFORMING ORGANIZATION REPORT NO.**
9. SPONSORING / MONITORING AGENCY NAME(S) AND ADDRESS(ES) Air Force Research Laboratory (AFMC) AFRL/RQR 5 Pollux Drive Edwards AFB, CA 93524-7048	**10. SPONSOR/MONITOR'S ACRONYM(S)**
	11. SPONSOR/MONITOR'S REPORT NUMBER(S) **AFRL-RQ-ED-VG-2016-145**

12. DISTRIBUTION / AVAILABILITY STATEMENT
Approved for Public Release; Distribution Unlimited. The U.S. Government is joint author of the work and has the right to use, modify, reproduce, release, perform, display, or disclose the work.

13. SUPPLEMENTARY NOTES
For presentation at ICOSAHOM16; Rio de Janeiro, Brazil (June 27th - July 1st, 2016)
PA Case Number: #16298; Clearance Date: 6/14/2016 Prepared in collaboration with ERC

14. ABSTRACT
Viewgraph/Briefing Charts

15. SUBJECT TERMS
N/A

16. SECURITY CLASSIFICATION OF:			**17. LIMITATION OF ABSTRACT**	**18. NUMBER OF PAGES**	**19a. NAME OF RESPONSIBLE PERSON** J. Koo
a. REPORT **Unclassified**	**b. ABSTRACT** **Unclassified**	**c. THIS PAGE** **Unclassified**	SAR	29	**19b. TELEPHONE NO** *(include area code)* N/A

Standard Form 298 (Rev. 8-98)
Prescribed by ANSI Std. 239.18

THE BLENDED FINITE ELEMENT METHOD FOR MULTI-FLUID PLASMA MODELING

Éder M. Sousa[1], Uri Shumlak[2]

[1]ERC INC., IN-SPACE PROPULSION BRANCH (RQRS)
AIR FORCE RESEARCH LABORATORY
EDWARDS AIR FORCE BASE, CA

[2]AEROSPACE AND ENERGETICS RESEARCH PROGRAM
UNIVERSITY OF WASHINGTON
SEATTLE, WA

ICOSAHOM16, June 27th - July 1st, 2016
Rio de Janeiro, Brazil

Outline

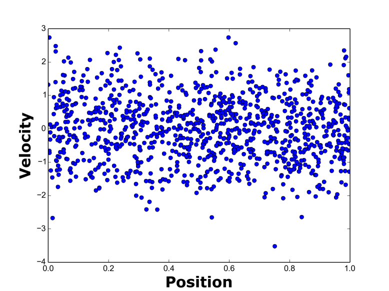

- 3-Dimensions + 3-Velocities
- Evolve the particles position and velocity
- e.g. Particle-In-Cell models

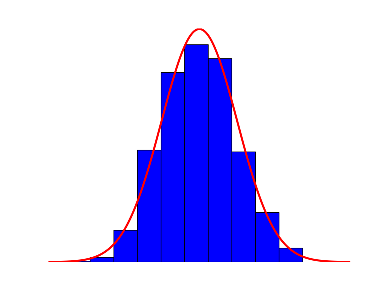

- Ensemble average of particles distribution, $f_s(\mathbf{x},\mathbf{v},t)$
- Evolve the distribution function
- e.g. Vlasov-Maxwell models

- Modeling each particle velocity and position is not practical.
- Instead an average is performed to give a statistical description.
- Calculate the number of particles per unit volume having approximately the velocity $\mathbf{v}$ near the position $\mathbf{x}$ and at time t, distribution function $f(\mathbf{v}, \mathbf{x}, \mathbf{t})$

$$\rho_s = m_s \int f_s(\mathbf{v}) d\mathbf{v}$$

$$\rho_s \mathbf{u}_s = m_s \int \mathbf{v} f_s(\mathbf{v}) d\mathbf{v}$$

$$\mathbb{P}_s = \mathbf{P}_s = m_s \int \mathbf{w}\mathbf{w} f_s(\mathbf{v}) d\mathbf{v}, \quad p_s = \frac{1}{3} m_s \int w^2 f_s(\mathbf{v}) d\mathbf{v}$$

$$\mathbf{H}_s = m_s \int \mathbf{w}\mathbf{w}\mathbf{w} f_s(\mathbf{v}) d\mathbf{v}, \quad \mathbf{h}_s = \frac{1}{2} m_s \int w^2 \mathbf{w} f_s(\mathbf{v}) d\mathbf{v}$$

$$\mathbf{w} = \mathbf{v} - \mathbf{u}_s$$

- The Boltzmann eqn:

$$\frac{\partial f_s}{\partial t} + \mathbf{v} \cdot \frac{\partial f_s}{\partial \mathbf{x}} + \frac{q_s}{m_s} \left(\mathbf{E} + \mathbf{v} \times \mathbf{B} \right) \cdot \frac{\partial f_s}{\partial \mathbf{v}} = \left. \frac{\partial f_s}{\partial t} \right|_c$$

- Take the 0^{th}, 1^{st}, 2^{nd} moments of the Boltzmann Eqn.

$$m_s \int \mathbf{v}^n \frac{\partial f_s}{\partial t} d\mathbf{v} + m_s \int \mathbf{v}^{n+1} \cdot \frac{\partial f_s}{\partial \mathbf{x}} d\mathbf{v} + q_s \int \mathbf{v}^n \left(\mathbf{E} + \mathbf{v} \times \mathbf{B} \right) \cdot \frac{\partial f_s}{\partial \mathbf{v}} d\mathbf{v} = m_s \int \mathbf{v}^n \left. \frac{\partial f_s}{\partial t} \right|_c d\mathbf{v}$$

- Each moment of the Boltzmann eqn gives an equation for the moment variable, and introduces the next higher moment variable
- This process can go on indefinitely

$$\frac{\partial \rho_s}{\partial t} + \nabla \cdot (\rho_s \mathbf{u}_s) = \left.\frac{\partial \rho_s}{\partial t}\right|_\Gamma$$

$$\frac{\partial \rho_s \mathbf{u}_s}{\partial t} + \nabla \cdot (\rho_s \mathbf{u}_s \mathbf{u}_s + p_s \mathbf{I} + \Pi_s) = \frac{\rho_s q_s}{m_s}(\mathbf{E} + \mathbf{u}_s \times \mathbf{B}) - \sum_{s*} \mathbf{R}_{s,s*} + \left.\frac{\partial \rho_s \mathbf{u}_s}{\partial t}\right|_\Gamma$$

$$\frac{\partial \varepsilon_s}{\partial t} + \nabla \cdot (((\varepsilon_s + p_s)\mathbf{I} + \Pi_s) \cdot \mathbf{u}_s + \mathbf{h}_s) = \frac{\rho_s q_s}{m_s} \mathbf{u}_s \cdot \mathbf{E} + \sum_{s*} Q_{s,s*} + \left.\frac{\partial \varepsilon_s}{\partial t}\right|_\Gamma$$

- System is truncated by relating higher moment variables to the lower ones
- The fluids are coupled to each other and to the electromagnetic fields through Maxwell's equations and interaction source terms.

Advantages of the Model

$$\textbf{Kinetic} \xrightarrow{\text{LTE, velocity moments}} \textbf{MFPM} \xrightarrow{\epsilon_o \to 0, \quad m_e \to 0} \textbf{MHD}$$

Ideal MHD model is valid when:

- High collisionality, $\tau_{ii}/\tau \ll 1$
- Small Larmor radius, $r_{Li}/L \ll 1$
- Low Resistivity, $\left(\frac{m_e}{m_i}\right)^{1/2} \left(\frac{r_{Li}}{L}\right)^2 \frac{\tau}{\tau_{ii}} \ll 1$

Multi-Fluid Plasma Model

- Less computationally expensive than kinetic models
- Multi-fluid effects become relevant at small spacial and temporal scales
- Finite electron mass and speed-of-light effects are included
- There is charge separation is modeled
- Displacement current effects are resolved in the MFPM

Outline

1. The Multi-fluid Plasma Model
2. Blended Finite Element Method
   - Blended Finite Element Method
   - Nodal Continuous Galerkin
   - Modal Discontinuous Galerkin
   - Model Verification
3. Results
   - 1D Soliton problem
   - Electromagnetic Plasma Shock Problem
4. Application

The MFPM has dispersive sources.

$$\frac{\partial \mathbf{Q}}{\partial t} + \frac{\partial \overleftrightarrow{\mathbf{F}}}{\partial \mathbf{x}} = \mathbf{S}$$

- The source Jacobian $\dfrac{\partial \mathbf{S}}{\partial \mathbf{Q}}$ has imaginary eigenvalues
- The equation system has dispersive sources
- The dispersion is physical (may be difficult to distinguish from numerical dispersion)
- This dispersion is due to plasma waves that result from ion and electron plasma interactions with electromagnetic fields
- An ideal numerical method for the MFPM should:
  - be high-order accurate
  - capture shocks
  - couple the flux and the sources
  - not impose strict time-step

Srinivasan et al, CCP 10 (2011)

- Solution to the electron and EM fields is smooth and does not shock

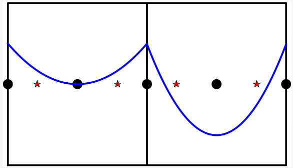

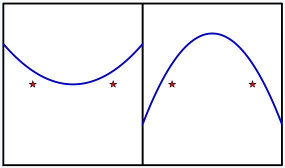

- Continuous Galerkin
- Electron fluid and EM fields

$$\mathbf{Q} = \sum_i \mathbf{q}_i v_i$$

- Discontinuous Galerkin
- Multiple ion and neutral fluids

$$\mathbf{Q} = \sum_i \mathbf{c}_i v_i$$

- For this implementation the balance law form is cast as

$$\frac{\partial \mathbf{Q}}{\partial t} + \frac{\partial \overleftrightarrow{\mathbf{F}}}{\partial \mathbf{Q}} \cdot \frac{\partial \mathbf{Q}}{\partial \mathbf{x}} = \mathbf{S} + \kappa \nabla^2 \mathbf{Q}_d$$

- Lagrange polynomials are used for basis functions, v_r

$$\int_\Omega v_r \frac{\partial \mathbf{Q}}{\partial t} dV = \mathcal{L}_r(\mathbf{Q}) = \int_\Omega v_r \mathbf{S} dV - \int_\Omega v_r \frac{\partial \overleftrightarrow{\mathbf{F}}}{\partial \mathbf{Q}} \cdot \frac{\partial \mathbf{Q}}{\partial \mathbf{x}} dV + \kappa \int_\Omega v_r \nabla^2 \mathbf{Q}_d dV$$

- θ-method time integration

$$\mathcal{R}(\mathbf{Q}^n) = \overleftrightarrow{\mathbf{M}} \frac{\mathbf{Q}^{n+1} - \mathbf{Q}^n}{dt} - \theta \mathcal{L}_r(\mathbf{Q}^{n+1}) - (1-\theta)\mathcal{L}_r(\mathbf{Q}^n) = 0$$

- $\theta = 0.5$ is used for 2^{nd} order accuracy

$$\overleftrightarrow{\mathbf{J}}(\mathbf{Q}^n) = \frac{\partial \mathcal{R}(\mathbf{Q}^n)}{\partial \mathbf{Q}^n}, \quad \overleftrightarrow{\mathbf{J}}(\mathbf{Q}^n)\Delta \mathbf{Q} = -\mathcal{R}(\mathbf{Q}^n), \quad \mathbf{Q}^{n+1} = \mathbf{Q}^n + \Delta \mathbf{Q}$$

Reddy, An Introduction to the Finite Element Method (2006)

$$\frac{\partial \mathbf{Q}}{\partial t} + \frac{\partial \overleftrightarrow{\mathbf{F}}}{\partial \mathbf{x}} = \mathbf{S}$$

- Legendre polynomials are used for basis functions, v_p
- The hyperbolic equation is multiplied by the basis function,

$$\int_\Omega v_p \frac{\partial \mathbf{Q}}{\partial t} dV = \mathcal{L}_p(\mathbf{Q}) = \int_\Omega v_p \mathbf{S} dV - \oint_{\partial\Omega} v_p \overleftrightarrow{\mathbf{F}} \cdot d\mathbf{A} + \int_\Omega \overleftrightarrow{\mathbf{F}} \cdot \nabla v_p dV$$

- Explicit Runge-Kutta time integration
- $CFL = c\Delta t/\Delta x \leq 1/(2p-1)$, p is the polynomial order

$$\mathbf{Q}^* = \mathbf{Q}^n + \Delta t \mathcal{L}_p(\mathbf{Q}^n),$$

$$\mathbf{Q}^{n+1} = \frac{1}{2}\mathbf{Q}^* + \frac{1}{2}\mathbf{Q}^n + \frac{1}{2}\Delta t \mathcal{L}_p(\mathbf{Q}^*).$$

Loverich et al, CCP 9 (2006)

$$\frac{\partial Q}{\partial t} + \frac{\partial Q}{\partial x} = 0, \qquad Q(x,0) = e^{-10(x-8)^2}, \qquad ||\Delta Q||_2 = \sqrt{\frac{1}{n}\sum_{i=1}^{n}(\hat{Q} - Q_i)^2}$$

Spatial Convergence

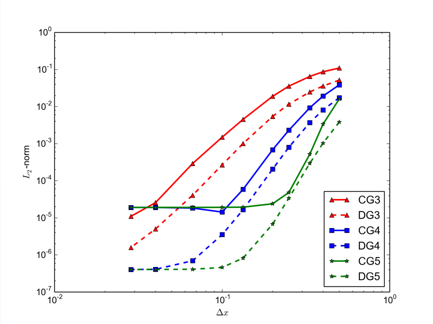

Temporal Convergence

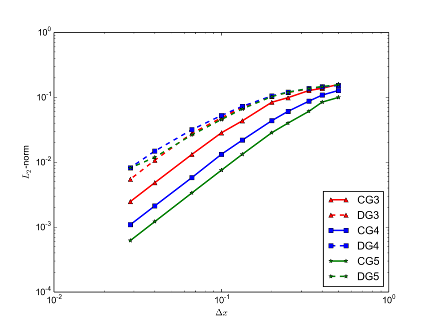

- Simulations at fixed time-step
- Simulations at fixed CFL=1

- 1D soliton is a two-fluid plasma problem
- The solution is smooth, therefore artificial dissipation can be small
- The simulation uses 512 second-order elements
- $B_z = 1.0$, $T_e = T_i = 0.01$, $\mathbf{u}_i = \mathbf{u}_e = \mathbf{0}$
- $n_e = n_i = 1.0 + e^{-10(x-6)^2}$

Baboolal, Math. and Comp. Sim. 55 (2001)

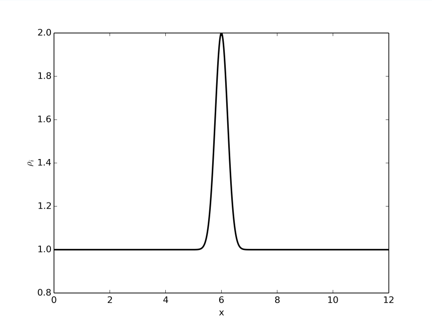

$$\frac{m_i}{m_e} = 1836, \ \frac{c}{c_{si}} = 1000\sqrt{2}, \text{ FV 5000 cells}$$

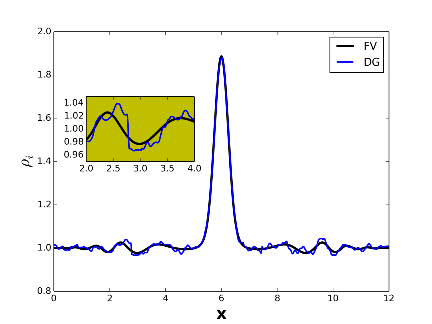

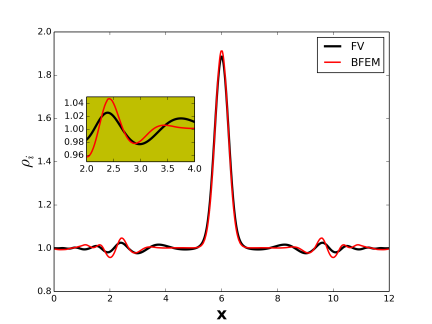

- DG Solution is very dispersive
- BFEM is less dissipative than the converged solution

Hakim et al, JCP 219 (2006)

case	m_i/m_e	c/c_{si}	DG time(s)	BFEM time (s)	BFEM cost over DG
1	25	$10/\sqrt{2}$	0.32	37.7	+11681%
2	100	$10/\sqrt{2}$	1.28	37.7	+2845%
3	500	$10/\sqrt{2}$	6.82	37.7	+452.8%
4	1000	$10/\sqrt{2}$	12.4	38.2	+208.1%
5	1836	$10/\sqrt{2}$	23.5	40.4	+71.91%
6	3672	$10/\sqrt{2}$	47.2	39.2	-16.95%
7	3672	$100/\sqrt{2}$	520	265	-49.04%
8	3672	$1000/\sqrt{2}$	5274	2735	-48.14%

- Per time-step explicit DG is faster than BFEM, but it requires many more time-steps
- BFEM is more efficient only when time-step are considerably larger than explicit DG

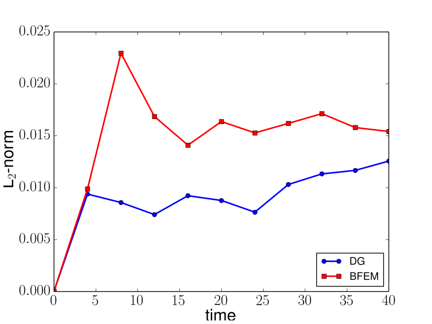

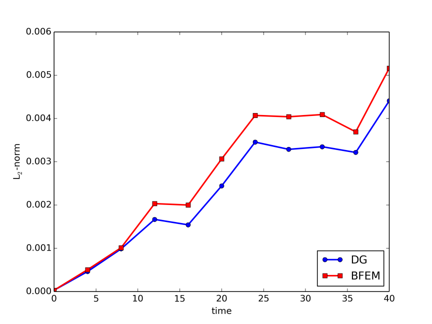

$m_i/m_e = 1836$ $m_i/m_e = 1$

- The BFEM seams to be less accurate than the DG implementation ($\sim 50\%$)
- When the mass ratio is one, the two methods have the same level of accuracy
- The discrepancy is due to the fact that the semi-implicit BFEM does not resolve the plasma frequency in this problem

- Fast rarefaction wave (FR), a slow compound wave (SC), a contact discontinuity (CD), a slow shock (SS), and another fast rarefaction wave (FR)
- The problem exhibits limits of MHD and multi-fluid behavior by changing the Larmor radius, r_L
  - MHD: $r_L \to 0$
  - Multi-fluid: $r_L \sim L$

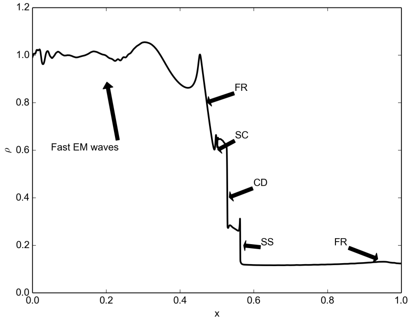

Brio and Wu, JCP 75 (1988)

- t=0.05/ω_{ci}, c/c_{si}=110, m_i/m_e=1836

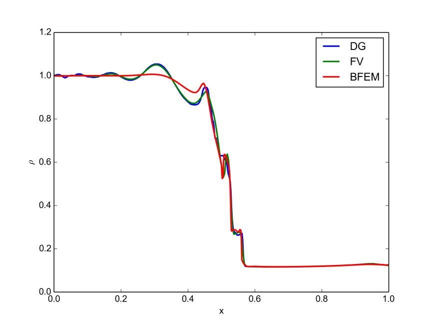

mass density

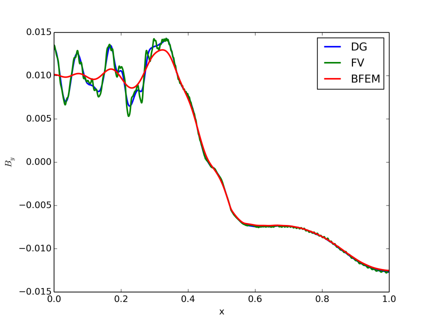

Magnetic field (y-comp.)

- The main features of the problem are captured by all three methods
- BFEM does not properly resolve the fast electromagnetic waves which require accurately resolving the electron dynamics

$$\Delta t_{max} = \min\left(\frac{\Delta x}{c_{se}}, \frac{\Delta x}{c_{si}}, \frac{\Delta x}{c}, \frac{0.1}{\omega_{ce}}, \frac{0.1}{\omega_{ci}}, \frac{0.1}{\omega_{pe}}, \frac{0.1}{\omega_{pi}}\right)$$

- Δt_{max} corresponds to the maximum value allowed for explicit methods based on the CFL condition
- $\Delta t = 42.9\Delta t_{max}$ is the maximum time step allowed by the BFEM due to ion dynamics

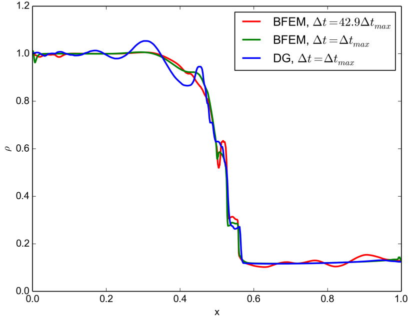

- Varying the artificial dissipation on the electron fluid, κ_e
- Wave-like behavior of the problem is better resolved
- Amplitude of the compound wave increases
- Right fast rarefaction wave is not visible

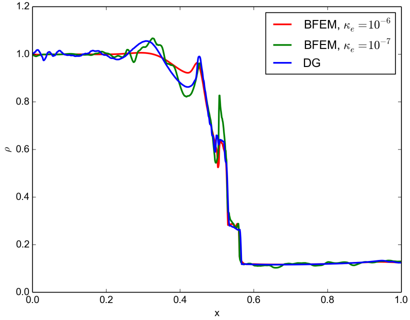

- Varying the artificial dissipation on the EM-field, κ_{EM}
- There is better agreement with the DG solution
- This reinforces the point that the wave-like behavior arises from the interaction of the electron fluid with the electromagnetic fields

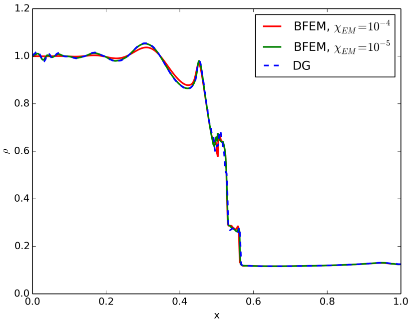

Outline

- Deuterium and tritium are heated and compressed to fusion conditions
- The compression is laser-driven
- Deuterium can accelerate faster than the tritium
- Low neutron yield measurements point towards separation
- The phenomenon is not captured by single-fluid plasma models

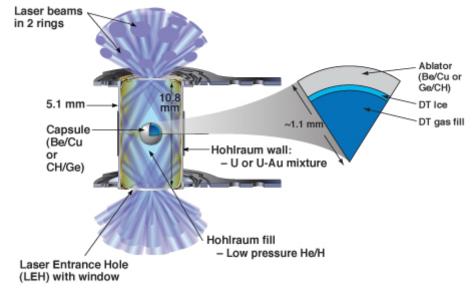

t=150ps

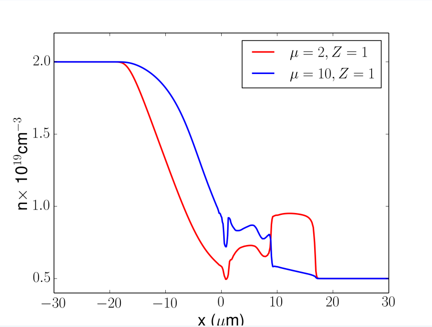

Electron CFL=1

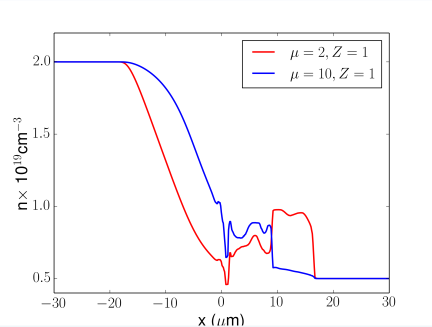

Electron CFL=20

- The ion species separation in both cases is the same although the solution behind the shock fronts differ

Bellei et al., PoP 20 (2013)

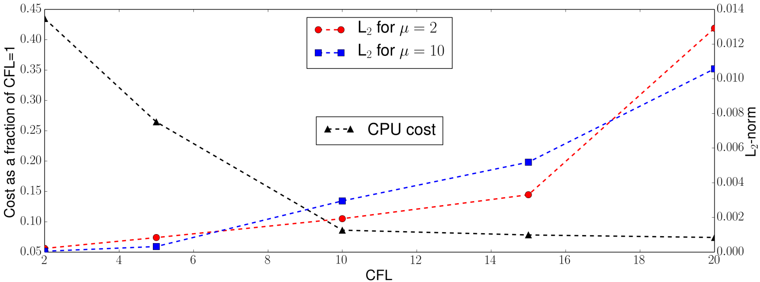

- The solution error increases as the computational time decreases.

Summary

- The blended finite element method (BFEM) is presented
  - DG spatial discretization with explicit Runge-Kutta time integration Ions and neutrals
  - CG spatial discretization with implicit Crank-Nicolson time integration for the electrons and EM fields
  - DG captures shocks and discontinuities
  - CG is efficient and robust for smooth solutions
- Physics-based decomposition of the algorithm yields numerical solutions that resolve the desired timescales
- DG method takes less computational time to advance the solution by one time-step, however Δt is much smaller than that of the BFEM
- Computational cost savings using the BFEM will only occur for relatively large implicit time-steps compared to explicit time-steps

Thank You.